Intercomparison of the Performance of Four Data Assimilation Schemes in a Limited-Area Model on Forecasts of an Extreme Rainfall Event over the Himalayas

Rakesh S* and Govindan Kutty[1]

[1]*Department of Earth and Space Sciences,*
Indian Institute of Space Science and Technology, Valiamala, 695547, India

Corresponding Author Address:

**Dr. Govindan Kutty M*
Associate Professor
Department of Earth and Space Sciences,
Indian Institute of Space Science and Technology, Valiamala, 695547, India
govind@iist.ac.in

Highlights

- The performance of four data assimilation systems are compared for a heavy rainfall event
- Non-cycled nested 4DVAR experiments outperformed the other experiments for rainfall forecasts
- Early merging of weather systems produced enhanced precipitation in EnKF experiments

Abstract

This study compares the performance of four data assimilation (DA) systems: Ensemble Adjustment Kalman Filter (EAKF), Variational (3DVAR/4DVAR), and Hybrid ensemble-3DVAR (HYBRID) in the Weather Research and Forecast (WRF) model. A heavy rainfall event that produced notorious floods in the Uttarakhand over the Himalayan region is considered. Observations are assimilated at every 6 h interval and all the conventional observations including cloud tracked-wind from the satellite are used. The forecast initialized from the analysis of four DA systems at different lead times is evaluated. A non-cycled nested assimilation strategy that provides advantages of increased resolution in the DA system is tested. The results indicate that 4DVAR experiments produce more skillful forecasts for wind while both 4DVAR and EAKF experiments show improvement for upper tropospheric temperature forecasts as compared to the other experiments. The evaluation of rainfall forecast depicts that the 4DVAR DA system has outperformed the other DA systems when the effect of high-resolution assimilation is mimicked in the system using the nested assimilation strategy. Further analysis of the event indicates that an early merging of the southward protruding trough with the westward-moving monsoon depression has resulted in stronger southeastward flow in EAKF and HYBRID experiments, which is suggested as a potential reason for enhanced precipitation over the Uttarakhand in both the experiments.

Keywords: Data Assimilation, Heavy Rainfall Event, WRF

1. Introduction

Data Assimilation (DA) methods are employed to improve the accuracy of initial conditions in a numerical weather prediction (NWP) model. Operational NWP models use variational (e.g, Parrish and Derber 1992, Kleist et al. 2009; Lorenc et al. 2000) and ensemble-based (e.g, Houtekamer and Mitchell 2005) DA algorithms to initialize the model forecasts. Three dimensional variational (3DVAR) approach estimates the minimum variance through iterative minimization of the cost function (Barker et al. 2004), while four-dimensional variational (4DVAR) scheme adds a time dimension in the variational framework through a linearized model and its adjoint (e.g., Rabier et al. 2000). One of the crucial factors that can influence the performance of a DA system is the prescription of background error covariance (BEC) matrix. The 3DVAR uses a time-invariant, climatological BEC, while the 4DVAR incorporates the time evolving flow-dependent information in the DA system, implicitly. On the other hand, the ensemble Kalman filter (EnKF) DA system follows probabilistic approach for assimilating observations with the model forecast that uses anisotropic, inhomogeneous flow-dependent BEC (Evensen 1994; Houtekamer and Mitchell 2001). The BEC in an EnKF DA system is estimated from the ensemble of nonlinear model forecasts, which carries the information about the “errors of the day”. The strategy of incorporating the ensemble estimated flow-dependent BEC in the variational framework is popularly known as Hybrid ensemble – variational DA system (“HYBRID”) (e.g; Hamill and Snyder 2000; Wang et al. 2008; Campbell et al. 2010). Compared to standalone ensemble-based DA system, HYBRID is computationally less expensive as it improves the state of the system with relatively smaller ensemble size. The effectiveness of HYBRID in improving the NWP forecasts are well documented (e.g., Buehner 2005; Kleist and Ide 2015; Kutty and Wang 2015; Kutty et al. 2018; Gogoi et al. 2020).

Previous studies have performed systematic intercomparison of the performance of DA systems in various NWP models. For instance, Whitaker et al. (2008) has shown that the analysis and forecast from EnKF are superior to that of 3DVAR in the operational global models of National Center for Environmental Prediction (NCEP) and Environmental Canada (Houtekamer and Mitchell 2005). Buehner et al. (2010) and Miyoshi et al. (2010) have shown that the performance of EnKF is comparable to that of 4DVAR in the operational models of Canadian and Japan Meteorological Agency (JMA). Wang et al. (2013) compared the performance of 3DVAR, EnKF and HYBRID DA system in the NCEP GFS and found that HYBRID produced more skillful forecast than EnKF and 3DVAR DA system. Zhang et al. (2011) has found similar results in the limited area regional models when the compared the performance of 3DVAR, 4DVAR and EnKF DA systems. Schwartz et al. (2013) suggested that the precipitation forecast initialized from HYBRID is better than from the standalone EnKF and 3DVAR. Chu et al. (2013) found that the performance of 4DVAR experiments is comparable to that of high-resolution 3DVAR experiments, which indicates that high resolution model forecasts are as important as the DA system for the precipitation forecasts. Despite the aforementioned studies, a comprehensive understanding of the performance of DA systems in the heavy rainfall events that involves multiscale dynamical interactions is elusive.

Extreme precipitation and flood episodes are quite frequent over Himalayan region and such high impact weather events are observed and studied extensively (e.g., Priya et al. 2015; Singh and Kumar 1997; Joshi and Kumar 2006; Joseph et al. 2015; Ranalkar et al. 2016;

Krishnamurti et al. 2017). Studies such as Rasmussen and Houze (2012) has shown that the extreme precipitation episodes over the Western Himalayas are multiscale in nature. During June 14 -17 of the year 2013, the Indian state, Uttarakhand experienced heavy rainfall and disastrous flooding thereafter. The event caused thousands of fatalities and extensive damages to the life and properties of the adjoining villages. In a study conducted by Vellore et al. (2016), it is found that extreme precipitation events over the Western Himalayas are often associated with southward penetrating large-scale westerly flow. Houze et al. (2017) suggested that the storm event is multiscale in nature and the presence of southward extended midlevel trough has provided a conducive environment for the development of the storm. Studies performed on the Uttarakhand heavy rainfall event using National Center for Medium Range Weather Forecasting (NCMRWF) Unified Model (NCUM) indicate improved performance in precipitation forecast when 4DVAR DA system is employed (Dube et al. 2014).

This study evaluates the performance of 3DVAR, 4DVAR, EAKF and HYBRID DA systems in Weather Research and Forecast (WRF) model for the extreme rainfall event over the Uttarakhand during 14 to 18 June 2013. Though the assimilation is performed on a coarser resolution domain, a non-cycled nested assimilation strategy is adopted to provide advantages of increased resolution in a computationally efficient manner (e.g., Cavallo et al. 2013; Torn 2010). This paper is organized as follows. Section 2 provides the experimental design. Section 3 describes major results and Section 4 and 5 provide discussion and conclusion of the paper, respectively.

2. Experimental design

The Advanced Weather Research and Forecast (ARW-WRF) of version 3.8.1 is used to investigate the performance of the DA systems. The WRF is a non-hydrostatic, fully compressible model with advanced parameterization schemes. This study employs Unified Noah Land Surface Model for surface parameterization, Rapid Radiative Transfer Model for longwave radiation calculation, Dudhia scheme for shortwave radiation calculation, WRF single-moment five-class for microphysics scheme, and Yonsei State University (YSU) scheme for planetary boundary layer parameterization. Simulations are performed in 27 km, 9 km, and 3 km resolution using two-way interactive nest with the assimilations performed on the outer domain. There are 36 non-uniformly spaced vertical levels with the model top at 50 hPa. The initial and lateral boundary conditions are generated from National Center for Environmental Prediction (NCEP) Global Forecast System (GFS) data available at 0.5^0 x 0.5^0 resolution. Observations available from the Global Telecommunication System (GTS) are assimilated in $\pm$ 3h interval assuming that all the observations are valid at the analysis time. The observations from various platforms are ingested including surface synoptic observation (SYNOP), buoys (BUOY), ships (SHIP), Radiosonde (RAOB), aircraft routine weather report (METAR), and wind reports from satellites (GEOAMV). Observation errors are obtained from the NCEP statistics and are assumed to be uncorrelated.

The 3DVAR, 4DVAR and HYBRID DA systems available in the WRF Data Assimilation system (WRFDA) are used in this study. The details regarding formulation and implementation of 3DVAR and 4DVAR is described in Barker et al. (2004) and Huang et al. (2009), respectively. The HYBRID DA system in WRFDA software uses extended control variable approach to incorporate ensemble covariance in 3DVAR cost function (Wang et al. 2008). Here, Ensemble Adjustment Kalman Filter (EAKF) from the Data Assimilation

Research Testbed (DART; Anderson 2001) is used to update the background ensembles in HYBRID DA system and also for the standalone EnKF DA system. Covariance localization and inflation is applied to maintain sufficient ensemble spread and avoid spurious correlations in the EAKF DA system. Gaspari and Cohn (1999) localization function has been used to control the effect of observations with half-widths of approximately 950 km in EAKF system. Initial inflation of 1.02 is applied to inflate the deviations from the ensemble mean using the adaptive inflation scheme (Anderson 2009) with a standard deviation of 0.6 and damping of 0.9.

The initial set of ensemble members are generated by adding randomly sampled perturbations to the initial conditions on 12 UTC 14 June 2013. The perturbations are the random draws from the distribution of the default background error covariance (“cv3” option) available in WRFDA system. The ensembles are then integrated forward in time for 12 hours to achieve model balance. The ensemble mean obtained at 00 UTC 15 June 2013 is used as the first guess for all the DA systems. Assimilation is then performed from 00 UTC 15 to 00 UTC 16 June 2013 every 6 h interval before the initializing the 48 h free forecast from the analysis at 00 UTC 16 June 2013.

2.1 Non-cycled nested assimilation

As indicated in the previous section, four sets of non-cycled nested assimilation experiments (Torn 2010) are performed for all the DA systems used in this study *viz*. 3DVAR-N, EAKF-N, HYBRID-N, and 4DVAR-N to provide advantages of increased resolution in a computationally efficient manner. The DA cycling is performed at 27 km horizontal grid spacing, which is too coarser to resolve the convective aspects of precipitation patterns of the event. To overcome this limitation, a non-cycled nested assimilation strategy is designed as follows. After completing the first analysis cycle at 27 km resolution, it is integrated forward in time to the next assimilation step using a two-interactive nested domain at 27 km, 9km, and 3 km horizontal grid spacing. It is to be noted that the innermost 3 km domain is centered on the Uttarakhand region. Once the forecast step is completed all the higher resolution runs are discarded and the assimilation is performed on the coarser resolution parent domain. Since the nesting strategy is two-way interactive, the outer domain will get benefitted from the high resolution innermost domain.

3. Results

3.1 Domain-wide comparison

The analyses from 3DVAR, 4DVAR, HYBRID and EAKF experiments are validated using root mean square (RMS) fit with respect to Radiosonde observations. The results from this section need to be treated with caution since assimilated observations are used for the verification of the analyses. Therefore, the RMS fit of analysis to observations are not depicting the analysis error, rather it shows how much each DA method draws its analysis closer to the observations. Figure 1 represents domain averaged vertical profiles of RMS fit of analysis to radiosonde observations for the mass and the wind variables for 3DVAR, EAKF, HYBRID and 4DVAR experiments. The analysis from EAKF fits more closely to the wind observations than 3DVAR, 4DVAR and HYBRID analyses. Compared to 3DVAR and 4DVAR, the analysis from HYBRID depicts a better fit to the wind observations. However, the analysis from the 3DVAR DA system depict a better fit to the temperature observations while for mixing ratio the EAKF analysis shows closer association to the observations. The prescription of background and observational error covariance plays an important role in determining the fit of analysis to observation. Since the specification of the observational error and the background are the same, the differences in RMS fit are due to differences in the background error covariance. Wang et al. (2013) has shown that the analysis fits better to the observations when the correlations scales (background error variances) are smaller (larger), and therefore, RMS fit may not reflect on the accuracy of forecasts generated from the analysis.

The root mean square error (RMSE) of horizontal wind components, temperature, and mixing ratio forecasts are validated with respect to radiosonde observations. The domain-averaged vertical profiles of RMSE at 24 h forecast lead time is shown in Figure 2. For wind, 4DVAR experiments produce more skillful forecasts as compared to the other experiments. The 4DVAR and EAKF experiments show improvements in the upper tropospheric temperature forecasts, and EAKF shows larger error near 800 hPa as compared to other experiments. Figure 3 illustrates the domain averaged RMSE for the four DA experiments at 48 h forecast lead time. Apparently, 4DVAR shows larger improvement in the meridional wind above about 500 hPa and below 300 hPa. Unlike the results from 24 h forecast lead time, EAKF experiment depicts larger error near the tropopause as compared to the other experiments, for zonal wind. As far as mixing ratio is concerned, EAKF and HYBRID experiments produce more skillful forecasts than 3DVAR and 4DVAR experiments over lower troposphere.

3.2 Rainfall

The geographical distribution of 24 h accumulated precipitation from TRMM satellite for day 1 and day 2 valid at 00 UTC June 17, 2013 and 00 UTC June 18, 2013, respectively, is shown in Figure 4. The TRMM satellite observation indicates that the rainfall is mostly over the

Uttarakhand state and the eastern parts of Himachal Pradesh for the first day while the precipitation bands are found to be shifted southeastward on the second day. Figure 5 shows 24 h accumulated precipitation for day 1 and day 2 simulated by 3DVAR, EAKF, HYBRID, and 4DVAR experiments. The EAKF and HYBRID experiments indicate that the rainfall is widely distributed over the Uttarakhand, and the northern regions of Himachal Pradesh. More specifically, two prominent precipitation maxima can be seen in EAKF experiment for day 1; one over the Uttarakhand and another one over the Himachal Pradesh (Figure 5c). The 4DVAR experiment simulated precipitation bands with a lower intensity and the precipitation maxima are located much south of the Uttarakhand state. For day 2, all the experiments except 4DVAR depict a southeastward shift of precipitation patterns as observed in TRMM satellite observations. Additionally, EAKF and HYBRID experiments overestimate the precipitation intensity, while 4DVAR run shows weak rainfall patterns as compared to the other experiments.

Figure 6 indicates that the position and intensity errors have reduced in all the experiments that adopted the non-cycled nested assimilation strategy, in general, and the largest improvement in day 2 precipitation forecast is observed for 4DVAR experiments (Figure 6f). It is worth noting that for non-cycled nested assimilation experiments, the intensity errors have considerably reduced in EAKF and HYBRID experiment as compared to the experiments without nesting. In the non-cycled nested assimilation, the spatial extent of precipitation in EAKF is larger than other experiments, and HYBRID run shows enhanced precipitation to the north of Uttarakhand.

To evaluate the precipitation forecasts quantitatively, verification statistics based on contingency table such as Equitable Threat Score (ETS), and Bias scores are employed. The

ETS value of 1 indicates perfect rainfall forecast by the experiments. The Bias score indicates the tendency of model to underpredict (when Bias score is less than 1) or overpredict an event (when Bias score is greater than 1). Figure 7 illustrates that among all the DA cycling experiments, 4DVAR-N shows the highest skill score for precipitation forecast for all the rainfall thresholds for both day 1 and day 2. For non-cycled nested assimilation experiments, rainfall forecast skill for day 1 has improved substantially in HYBRID-N experiment as compared to its corresponding non-nested assimilation experiment. The EAKF experiments have overestimated day1 and day 2 rainfall forecasts, however with a reduced intensity estimation error for day 1 precipitation in EAKF-N experiment. Barring that, using the non-cycled nested assimilation strategy is found to be not very effective in EAKF experiments. On the other hand, 3DVAR-N experiment shows higher skill scores at lower thresholds as compared to 3DVAR. Overall, the results indicate that convection-permitting resolution is inevitable for the accurate precipitation forecast and the 4DVAR DA system has outperformed other DA systems when the effect of high-resolution assimilation is mimicked in the system using the nested assimilation strategy.

4. Discussion

The primary synoptic scale factor that is associated with the devastating rainfall over the Uttarakhand during June 2013 is the southward extending midlevel trough that eventually merged with westward migrating monsoon low. The accuracy in the precipitation placement and intensity forecast depends on the accuracy in the depiction of synoptic-scale flow pattern in the DA analysis and forecast. Figure 8 shows the geopotential heights at 850 hPa in the analysis valid at 00 UTC of 16 June 2013 of 3DVAR, EAKF, HYBRID, and 4DVAR, which indicates that position of the trough simulated in each experiments are distinctly different.

This could be the potential reason for the observed variations in the position and intensity of precipitation forecast over the Uttarakhand. To understand how the variations in the analysis reflected in the forecast, the evolution of geopotential height at 850 hPa level in the forecasts initialized from each of the analysis is shown in Figure 9. While EAKF and HYBRID experiments depicted an early merging of southward protruding trough with the westward moving monsoon depression, the forecast from 4DVAR analysis indicates that the merging weather system occurred by June 17. The merging of weather systems and northward shift in the position of trough created a strong southwesterly flow over the Uttarakhand by 16 June 2013 in the EAKF experiment, which is proposed as the reason for enhanced precipitation in EAKF run during the first 24 h model forecast (Figure 5c). The enhanced magnitude and northward shift in the position of trough in EAKF experiment during the later hours of forecast can be attributed as the reason for stronger precipitation band. Figure 10 shows the vertical cross-section plot of specific humidity overlaid with the wind vectors during 18 UTC of 16 June 2013. Vertical extension of moisture column is more pronounced in EAKF and 3DVAR run as compared to 4DVAR experiment. Furthermore, EAKF indicates stronger vertical updraft along Himalayan escarpment as compared to other experiments, which could be due to the proximity of the trough over the Uttarakhand region.

5. Conclusion

The performance of four DA systems viz. 3DVAR, EAKF, HYBRID, and 4DVAR in Weather Research and Forecast (WRF) model during a heavy rainfall event over the Himalayas is compared. The accuracy of forecast initialized from the four DA systems at different lead times is examined. A non-cycled nested assimilation strategy that provides advantages of increased resolution in a computationally efficient manner in a DA system is tested.

Results indicate that the analysis from EAKF fits more closely to the wind observations than 3DVAR, 4DVAR and HYBRID analyses. Compared to 3DVAR and 4DVAR, the analysis from HYBRID depicts a better fit to the wind observations. For 24 h wind forecasts, the 4DVAR experiments are found to be more skillful as compared to the other experiments while for upper tropospheric temperature forecasts, both 4DVAR and EAKF experiments outperforms other experiments. For 48 h forecasts, 4DVAR shows larger improvements in the meridional wind and unlike the results from 24 h forecast lead time, EAKF experiment depicts larger error near the tropopause as compared to the other experiments. The forecasts initialized from EAKF and HYBRID DA systems produce more skillful forecasts for mixing ratio than that from 3DVAR and 4DVAR over lower troposphere. The EAKF experiments overestimates rainfall intensity, while the 4DVAR experiments underestimates the precipitation in both forecast days. The spatial patterns of precipitation and quantitative skill scores indicate that the non-cycled nested assimilation strategy has significantly improved the forecast skill scores, especially for 4DVAR experiments. Further analysis indicates that an early merging of southward protruding trough with the westward moving monsoon depression has resulted in stronger southeastward flow in EAKF and HYBRID experiments, which is suggested as a potential reason for enhanced precipitation over the Uttarakhand in both the experiments.

The present study is an initial effort to broaden our understanding on the performance of data assimilation system during an extreme rainfall event that occurred over Himalayas. The data assimilation cycling is performed in relatively coarser resolution. The skill of data assimilations systems will improve significantly, when high-resolution background and observations such as that from radar are used. More systematic comparisons during such weather events are required for understanding the fundamental differences that are significant for the performance of data assimilation systems. Future studies in this direction are warranted.

Acknowledgement:

The NCEP global forecast system analyses and forecasts data that is utilized in this study are openly available in the repository https://rda.ucar.edu at https://doi.org/10.5065/D65Q4TSG. Data assimilation is performed using observations derived from NCEP ADP Global Upper Air and Surface Weather Observations archived in the https://rda.ucar.edu at https://doi.org/10.5065/Z83F-N512.

References:

*Anderson, J., 2009: Spatially and temporally varying adaptive covariance inflation for ensemble filters. Tellus A: Dynamic meteorology and oceanography, **61,** 72-83.*

*Anderson, J. L., 2001: An ensemble adjustment Kalman filter for data assimilation. Monthly Weather Review, **129,** 2884-2903.*

*Barker, D. M., W. Huang, Y.-R. Guo, A. Bourgeois, and Q. Xiao, 2004: A three-dimensional variational data assimilation system for MM5: Implementation and initial results. Monthly Weather Review, **132,** 897-914.*

*Buehner, M., 2005: Ensemble-derived stationary and flow-dependent background-error covariances: Evaluation in a quasi-operational NWP setting. Quarterly Journal of the Royal Meteorological Society, **131,** 1013-1043.*

*Buehner, M., P. Houtekamer, C. Charette, H. L. Mitchell, and B. He, 2010: Intercomparison of variational data assimilation and the ensemble Kalman filter for global deterministic NWP. Part I: Description and single-observation experiments. Monthly Weather Review, **138,** 1550-1566.*

*Campbell, W. F., C. H. Bishop, and D. Hodyss, 2010: Vertical covariance localization for satellite radiances in ensemble Kalman filters. Monthly Weather Review, **138,** 282-290.*

*Cavallo, S. M., R. D. Torn, C. Snyder, C. Davis, W. Wang, and J. Done, 2013: Evaluation of the Advanced Hurricane WRF Data Assimilation System for the 2009 Atlantic Hurricane Season. Monthly Weather Review, **141,** 523-541.*

*Chu, K., Q. Xiao, and C. Liu, 2013: Experiments of the WRF three-/four-dimensional variational (3/4DVAR) data assimilation in the forecasting of Antarctic cyclones. Meteorology and Atmospheric Physics, **120,** 145-156.*

*Dube, A., R. Ashrit, A. Ashish, K. Sharma, G. Iyengar, E. Rajagopal, and S. Basu, 2014: Forecasting the heavy rainfall during Himalayan flooding—June 2013. Weather and Climate Extremes, **4,** 22-34.*

Evensen, G., 1994: Sequential data assimilation with a nonlinear quasi-geostrophic model using Monte Carlo methods to forecast error statistics. Journal of Geophysical Research: Oceans, **99,** 10143-10162.

Gaspari, G., and S. E. Cohn, 1999: Construction of correlation functions in two and three dimensions. Quarterly Journal of the Royal Meteorological Society, **125,** 723-757.

Gogoi, R. B., G. Kutty, V. Rakesh, and A. Borogain, 2020: Comparison of the Performance of Hybrid ETKF-3DVAR and 3DVAR Data Assimilation Systems on Short-Range Forecasts during Indian Summer Monsoon Season in a Limited-Area Model. Pure and Applied Geophysics**,** 1-20.

Hamill, T. M., and C. Snyder, 2000: A hybrid ensemble Kalman filter–3D variational analysis scheme. Monthly Weather Review, **128,** 2905-2919.

Houtekamer, P. L., and H. L. Mitchell, 2001: A sequential ensemble Kalman filter for atmospheric data assimilation. Monthly Weather Review, **129,** 123-137.

Houtekamer, P. L., and H. L. Mitchell, 2005: Ensemble Kalman filtering. Quarterly Journal of the Royal Meteorological Society, **131,** 3269-3289.

Houze, R., L. McMurdie, K. Rasmussen, A. Kumar, and M. Chaplin, 2017: Multiscale aspects of the storm producing the June 2013 flooding in Uttarakhand, India. Monthly Weather Review, **145,** 4447-4466.

Huang, X.-Y., and Coauthors, 2009: Four-Dimensional Variational Data Assimilation for WRF: Formulation and Preliminary Results. Monthly Weather Review, **137,** 299-314.

Joseph, S., and Coauthors, 2015: North Indian heavy rainfall event during June 2013: diagnostics and extended range prediction. Climate dynamics, **44,** 2049-2065.

Joshi, V., and K. Kumar, 2006: Extreme rainfall events and associated natural hazards in Alaknanda valley, Indian Himalayan region. Journal of Mountain Science, **3,** 228-236.

Kleist, D. T., and K. Ide, 2015: An OSSE-based evaluation of hybrid variational–ensemble data assimilation for the NCEP GFS. Part I: System description and 3D-hybrid results. Monthly Weather Review, **143,** 433-451.

Kleist, D. T., D. F. Parrish, J. C. Derber, R. Treadon, W.-S. Wu, and S. Lord, 2009: Introduction of the GSI into the NCEP global data assimilation system. Weather and Forecasting, **24,** 1691-1705.

Krishnamurti, T., and Coauthors, 2017: March of buoyancy elements during extreme rainfall over India. Climate dynamics, **48,** 1931-1951.

Kutty, G., and X. Wang, 2015: A Comparison of the Impacts of Radiosonde and AMSU Radiance Observations in GSI Based 3DEnsVar and 3DVar Data Assimilation Systems for NCEP GFS. Advances in Meteorology, **2015**.

Kutty, G., R. Muraleedharan, and A. P. Kesarkar, 2018: Impact of Representing Model Error in a Hybrid Ensemble-Variational Data Assimilation System for Track Forecast of Tropical Cyclones over the Bay of Bengal. Pure and Applied Geophysics, **175,** 1155-1167.

Lorenc, A., and Coauthors, 2000: The Met. Office global three-dimensional variational data assimilation scheme. Quarterly Journal of the Royal Meteorological Society, **126,** 2991-3012.

Miyoshi, T., Y. Sato, and T. Kadowaki, 2010: Ensemble Kalman filter and 4D-Var intercomparison with the Japanese operational global analysis and prediction system. Monthly Weather Review, **138,** 2846-2866.

Parrish, D. F., and J. C. Derber, 1992: The National Meteorological Center's spectral statistical-interpolation analysis system. Monthly Weather Review, **120,** 1747-1763.

Priya, P., M. Mujumdar, T. P. Sabin, P. Terray, and R. Krishnan, 2015: Impacts of Indo-Pacific Sea Surface Temperature Anomalies on the Summer Monsoon Circulation and Heavy Precipitation over Northwest India–Pakistan Region during 2010. Journal of Climate, **28,** 3714-3730.

Rabier, F., H. Järvinen, E. Klinker, J.-F. Mahfouf, and A. Simmons, 2000: The ECMWF operational implementation of four-dimensional variational assimilation. I: Experimental results with simplified physics. Quarterly Journal of the Royal Meteorological Society, **126,** 1143-1170.

Ranalkar, M. R., H. S. Chaudhari, A. Hazra, G. Sawaisarje, and S. Pokhrel, 2016: Dynamical features of incessant heavy rainfall event of June 2013 over Uttarakhand, India. Natural Hazards, **80,** 1579-1601.

Rasmussen, K. L., and R. A. Houze, 2012: A Flash-Flooding Storm at the Steep Edge of High Terrain: Disaster in the Himalayas. Bulletin of the American Meteorological Society, ***93,*** *1713-1724.*

Schwartz, C. S., Z. Liu, X.-Y. Huang, Y.-H. Kuo, and C.-T. Fong, 2013: Comparing limited-area 3DVAR and hybrid variational-ensemble data assimilation methods for typhoon track forecasts: Sensitivity to outer loops and vortex relocation. Monthly Weather Review, ***141,*** *4350-4372.*

Singh, P., and N. Kumar, 1997: Effect of orography on precipitation in the western Himalayan region. Journal of Hydrology, ***199,*** *183-206.*

Torn, R. D., 2010: Performance of a mesoscale ensemble Kalman filter (EnKF) during the NOAA high-resolution hurricane test. Monthly Weather Review, ***138,*** *4375-4392.*

Vellore, R. K., and Coauthors, 2016: Monsoon-extratropical circulation interactions in Himalayan extreme rainfall. Climate dynamics, ***46,*** *3517-3546.*

Wang, X., D. M. Barker, C. Snyder, and T. M. Hamill, 2008: A hybrid ETKF-3DVAR data assimilation scheme for the WRF model. Part I: Observing system simulation experiment. Monthly Weather Review, ***136,*** *5116-5131.*

Wang, X., D. Parrish, D. Kleist, and J. Whitaker, 2013: GSI 3DVar-Based Ensemble–Variational Hybrid Data Assimilation for NCEP Global Forecast System: Single-Resolution Experiments. Monthly Weather Review, ***141,*** *4098-4117.*

Whitaker, J. S., T. M. Hamill, X. Wei, Y. Song, and Z. Toth, 2008: Ensemble data assimilation with the NCEP global forecast system. Monthly Weather Review, ***136,*** *463-482.*

Zhang, M., F. Zhang, X.-Y. Huang, and X. Zhang, 2011: Intercomparison of an Ensemble Kalman Filter with Three- and Four-Dimensional Variational Data Assimilation Methods in a Limited-Area Model over the Month of June 2003. Monthly Weather Review, ***139,*** *566-572.*

Figures:

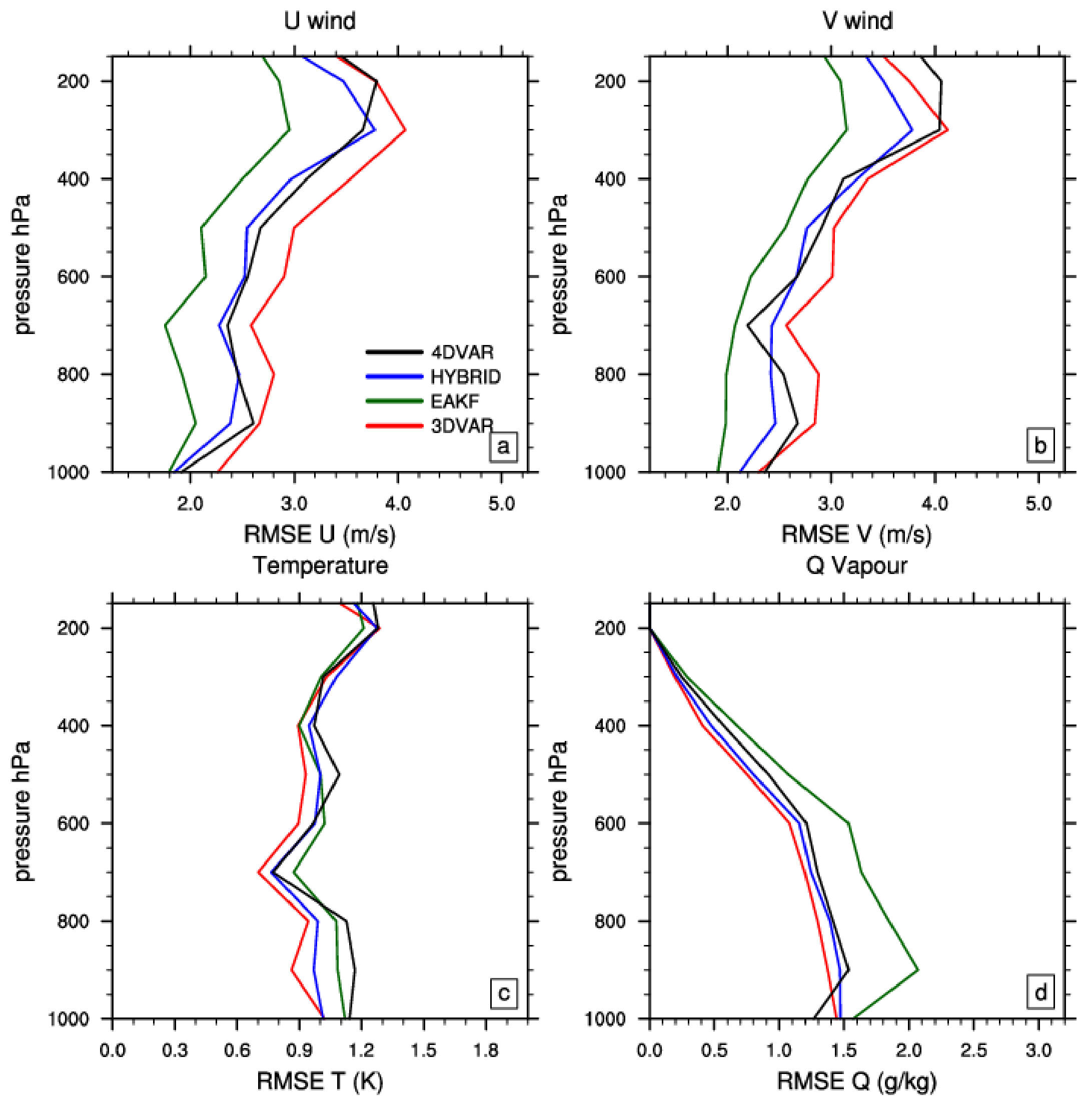

Figure 1: Domain averaged profiles of Root Mean Square (RMS) fit of analysis to Radiosonde observations for (a) Zonal wind (b) Meridional wind (c) Temperature, (d) Mixing ratio. Red, green, blue and black are for 3DVAR, EAKF, HYBRID, and 4DVAR experiments, respectively

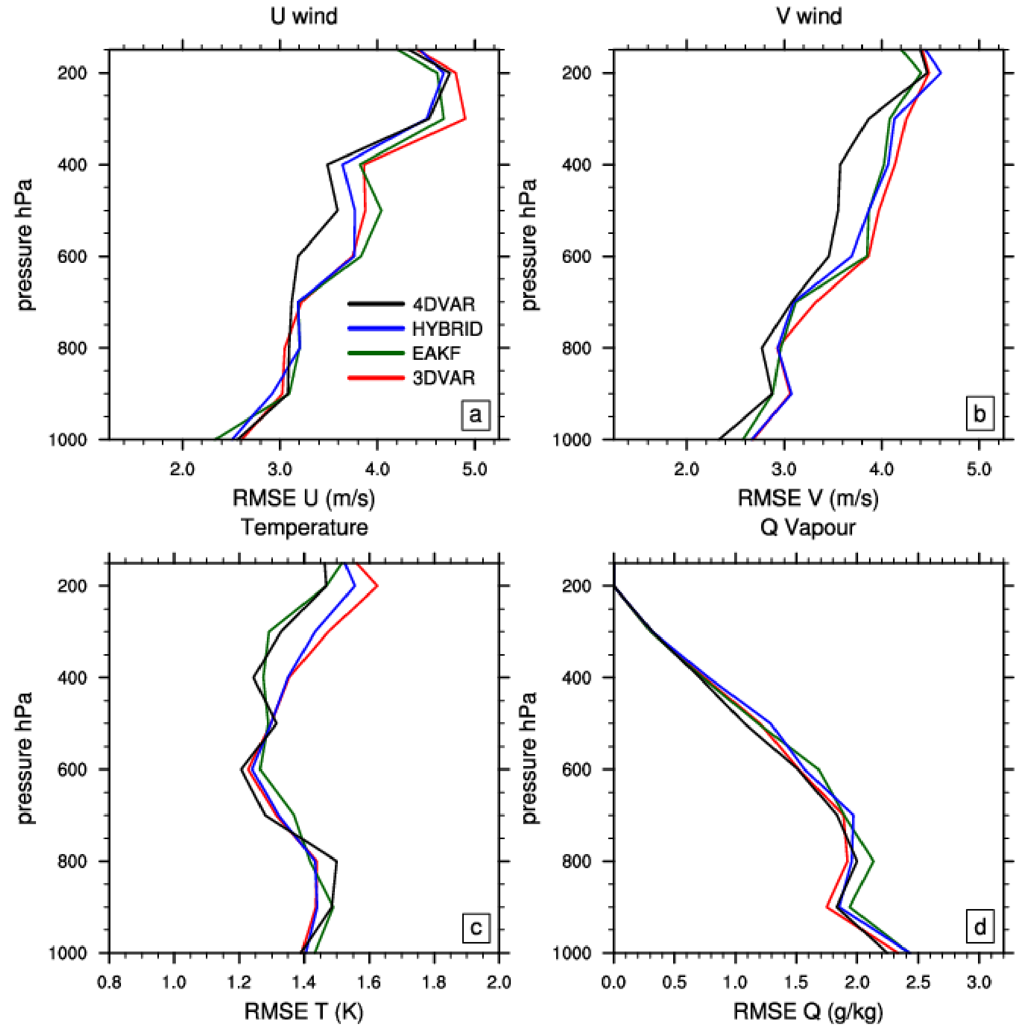

422

423

424 **Figure 2:** Vertical profiles of RMSE with respect to Radiosonde observations for 24 h forecasts
425 for (a) Zonal wind (b) Meridional wind (c) Temperature, (d) Mixing ratio. Red, green, blue and
426 black are for 3DVAR, EAKF, HYBRID, and 4DVAR experiments, respectively

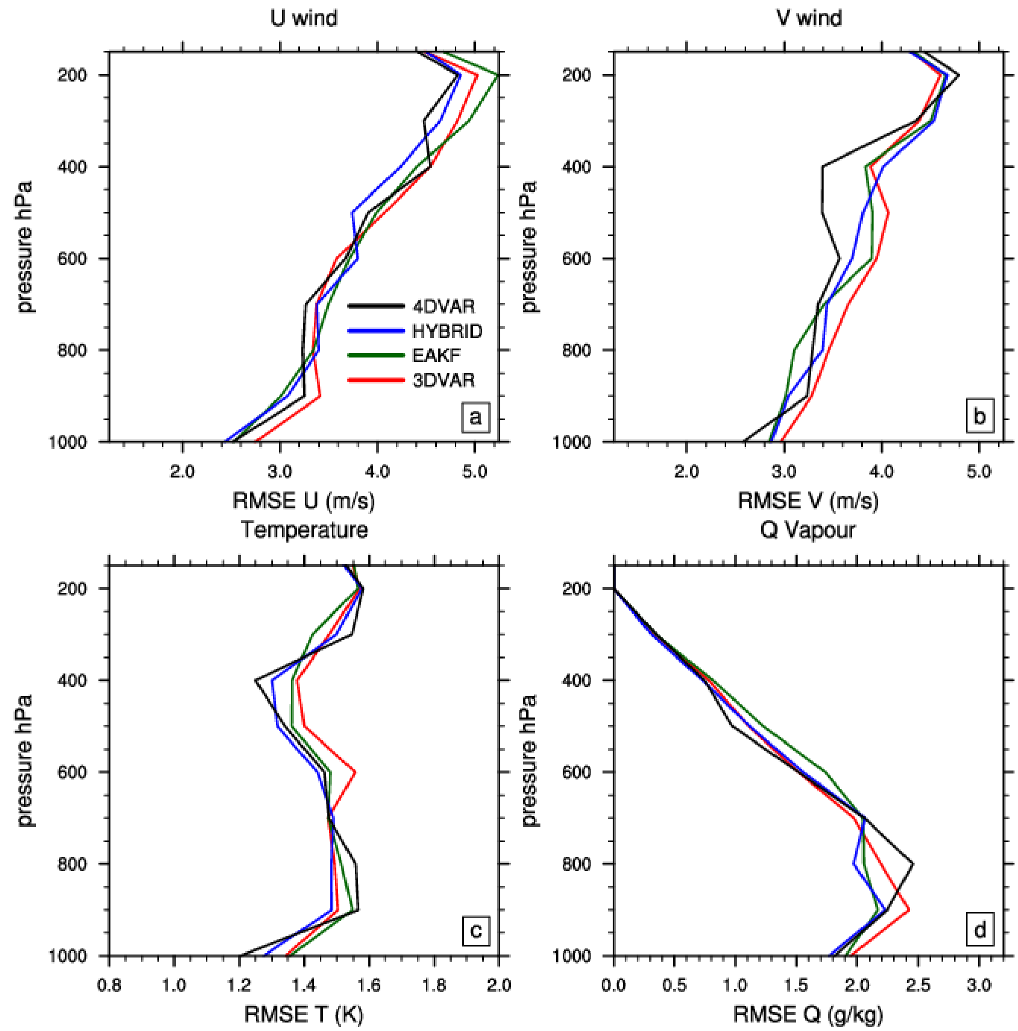

Figure 3: Same as in Figure 2, but for 48 h forecast

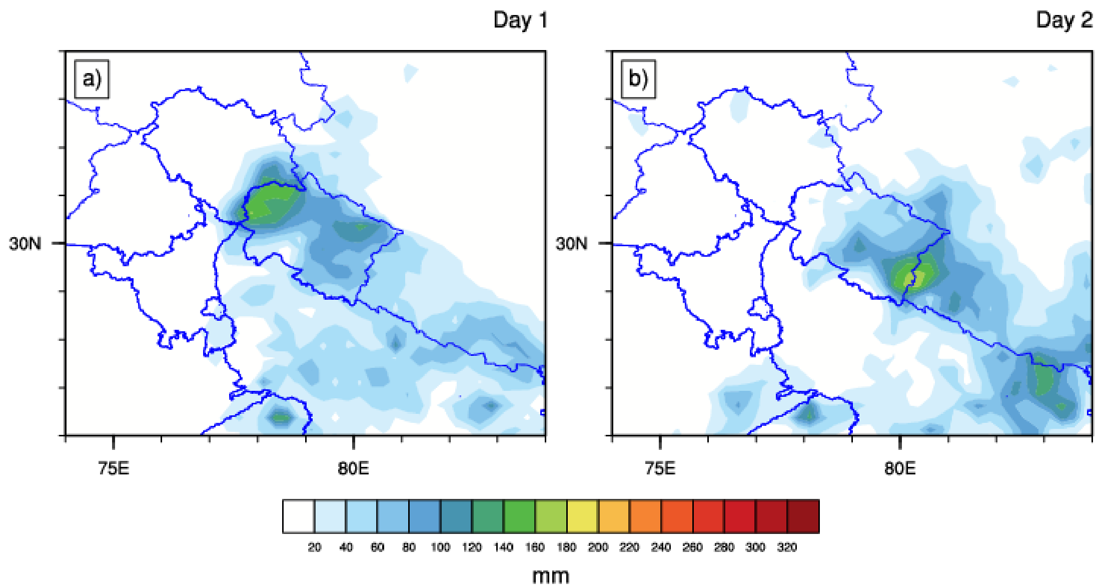

Figure 4: Geographical distribution of 24 h accumulated precipitation from TRMM satellite observations valid at (a) 00 UTC June 17, 2013 and (b) 00 UTC June 18, 2013.

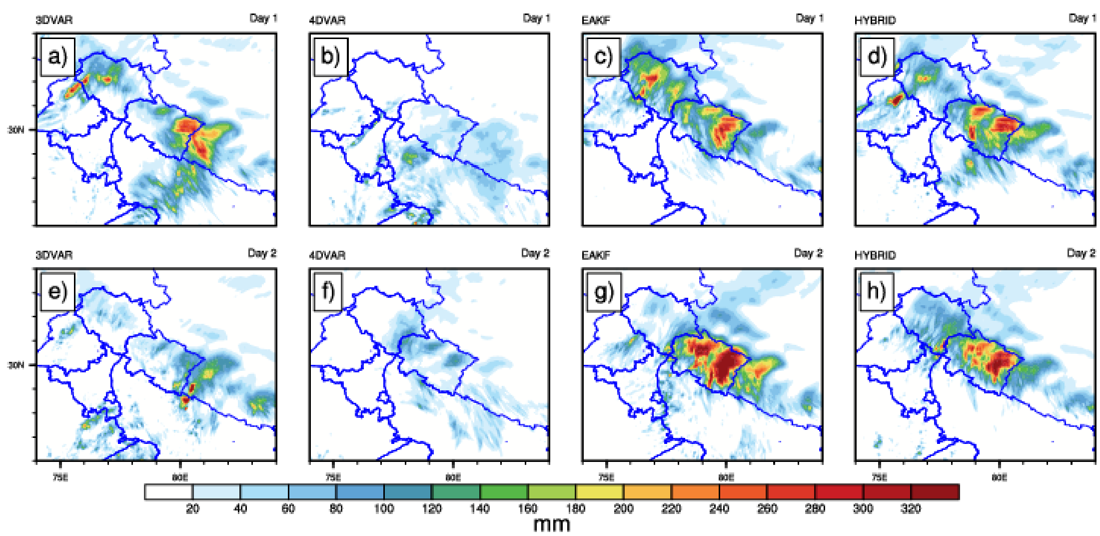

Figure 5: Geographical distribution of 24 h accumulated precipitation valid at (top panel: a-d) 00 UTC June 17, 2013 and (bottom panel: e-h) 00 UTC June 18, 2013, respectively, for (a,e) 3DVAR (b,f) 4DVAR (c,g) EAKF (d,h) HYBRID experiments.

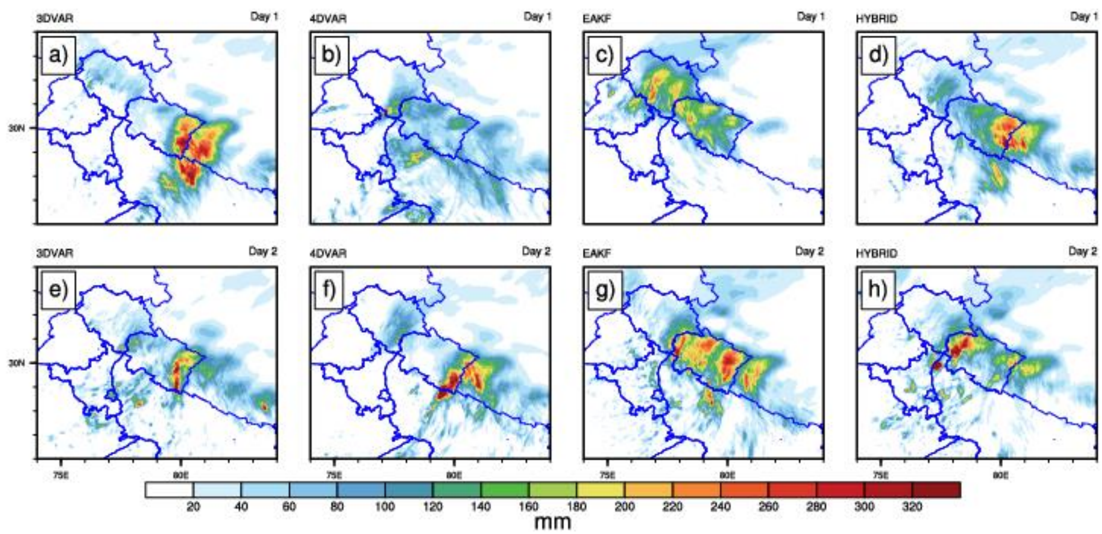

Figure 6: Same as in Figure 5, but for non-cycled nested assimilation experiments

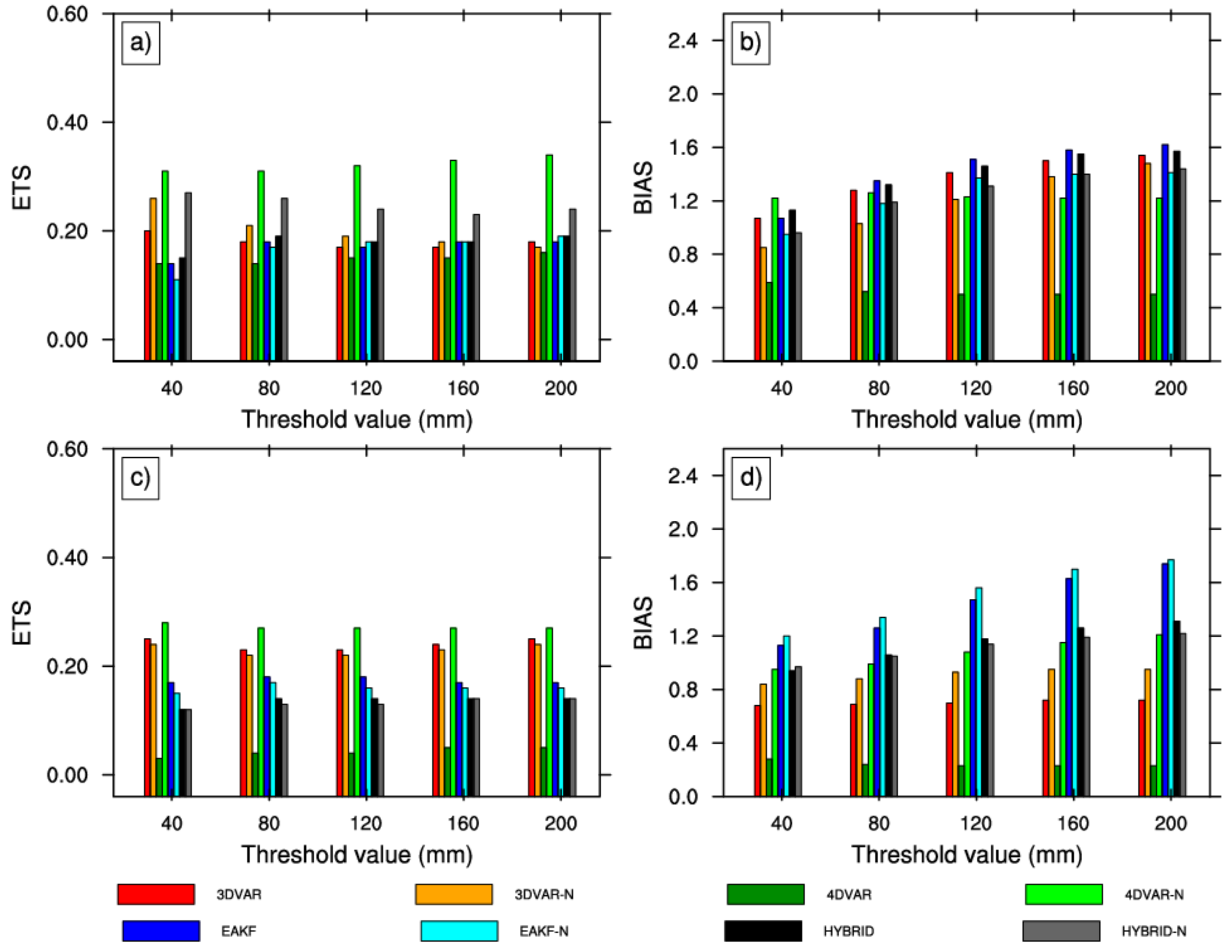

Figure 7: The ETS and Bias Scores for rainfall forecasts valid at (top panel: a, b) 00 UTC June 17, 2013 and (bottom panel: c, d) 00 UTC June 18, 2013. Red, green, blue, black, orange, light green, cyan, and grey are for 3DVAR, 4DVAR, EAKF, HYBRID, 3DVAR-N, 4DVAR-N, EAKF-N, HYBRID-N experiments, respectively

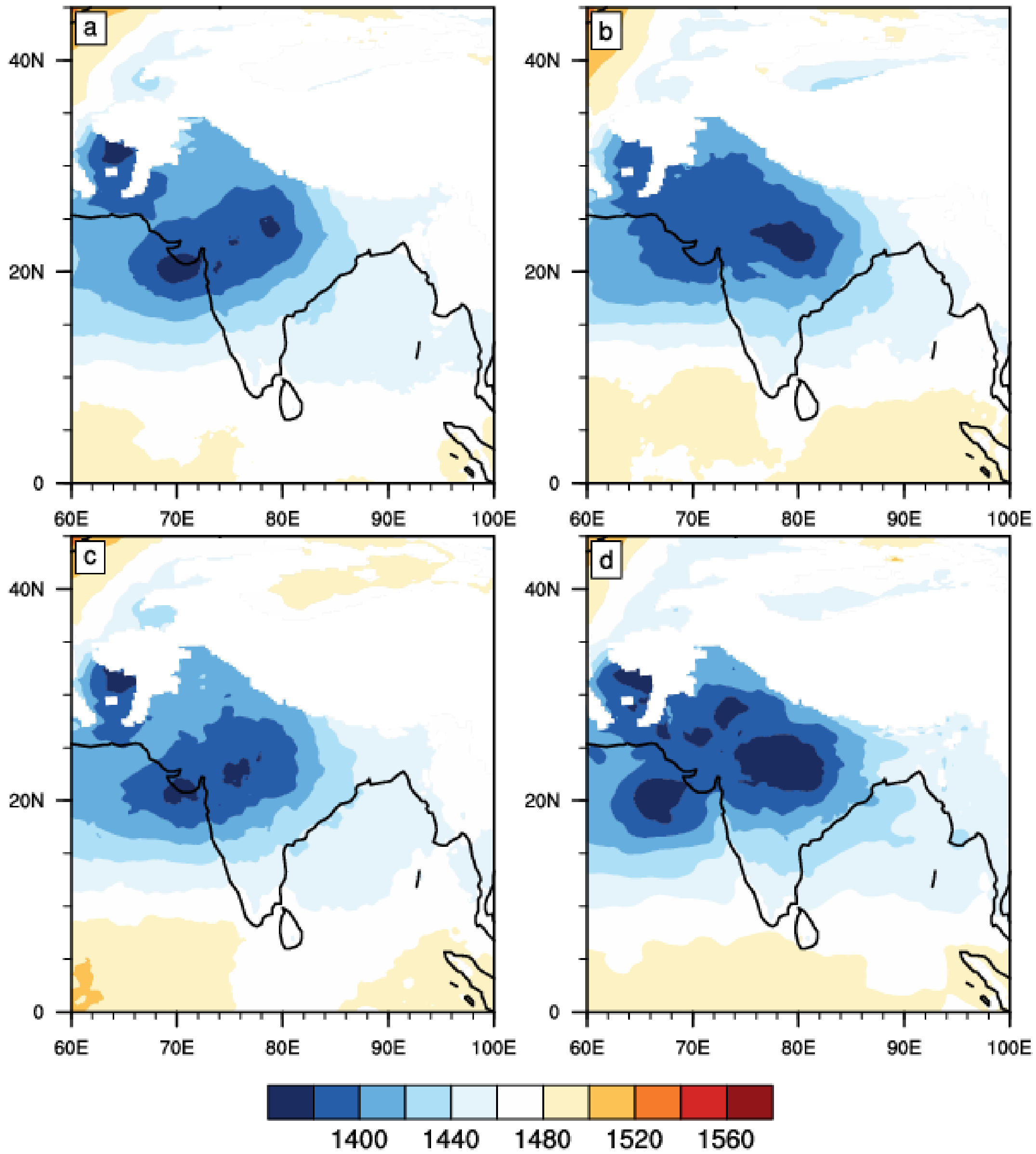

453

454

455 **Figure 8:** Spatial distribution of geopotential height at 850 hPa from the analysis of (a) 3DVAR
456 (b) EAKF (c) HYBRID (d) 4DVAR valid at 00 UTC of 16 June 2013

457

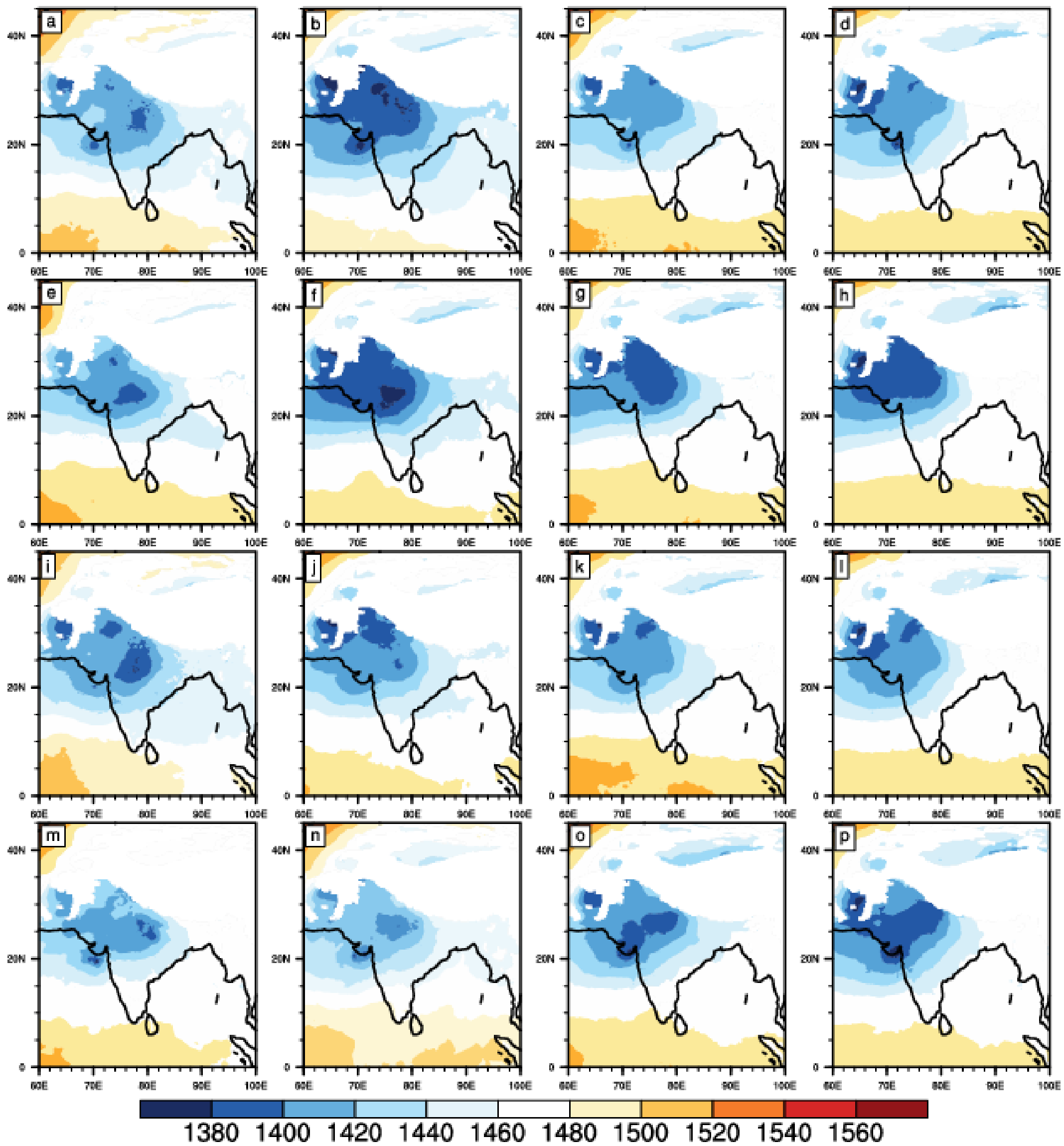

Figure 9: Time evolution of geopotential height at 850 hPa forecasts for (first row: a-d) 3DVAR (second row: e-h) EAKF (third row: i-l) HYBRID (fourth row: m-p) 4DVAR experiments at 0 h, 6h, 12h, and 18 h forecast.

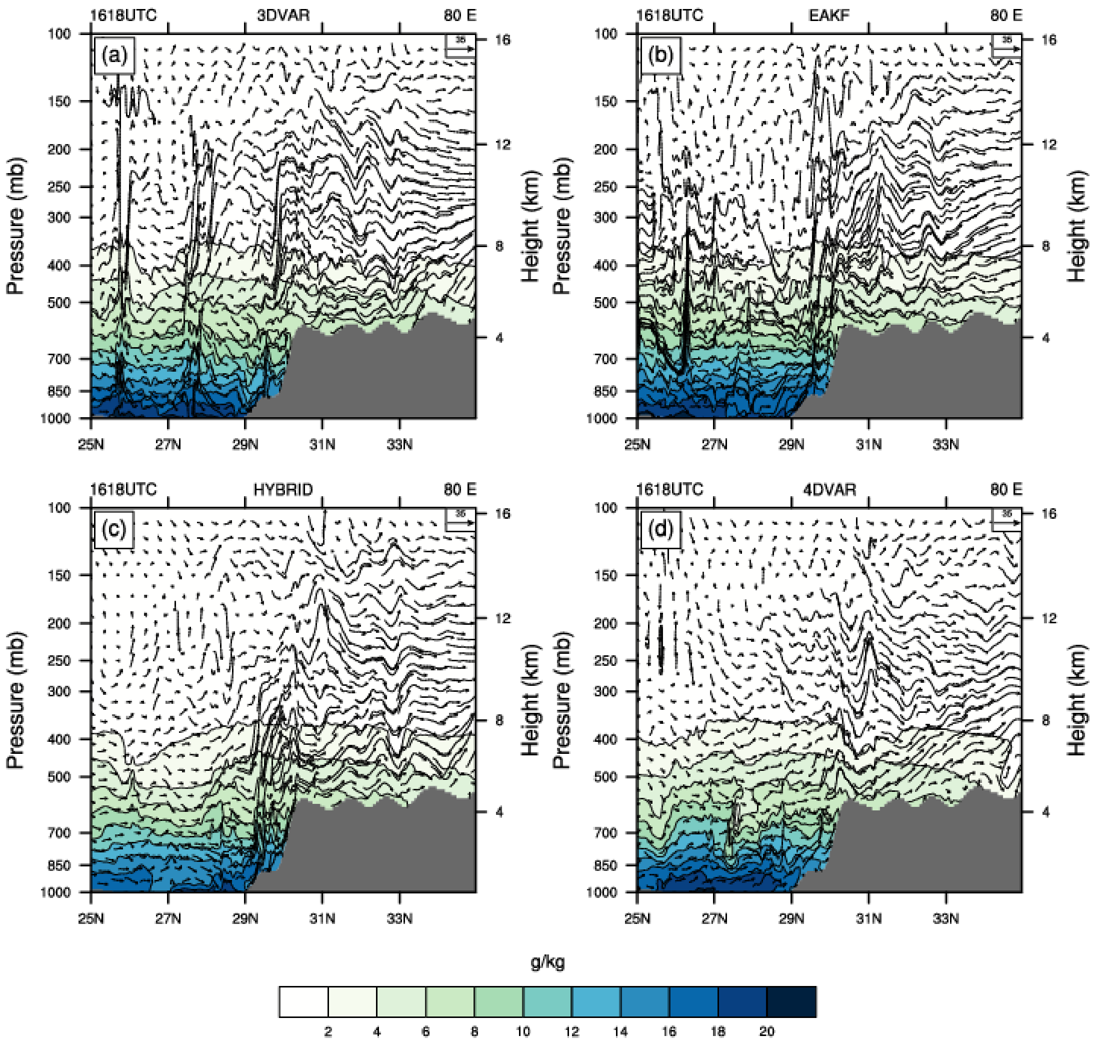

Figure 10: Vertical cross section of mixing ratio (shaded) overlaid with the wind vectors for (a) 3DVAR (b) EAKF (c) HYBRID (d) 4DVAR experiments valid at 18 UTC of 16 June 2013.